ELSEVIER

Polymer 40 (1999) 5407–5413

polymer

Thermally initiated cure kinetic of bismaleimides containing poly(dimethylsiloxane)

Wang Chun-Shan*, Leu Tsu-Shang

Department of Chemical Engineering, National Cheng Kung University, Tainan 701, Taiwan

Received 21 July 1998; received in revised form 6 October 1998; accepted 19 October 1998

Abstract

A series of maleimide-terminated amorphous poly(dimethylsiloxanes) were synthesized from amino-terminated poly(dimenthylsiloxanes) with various molecular weights. The oligomers were characterized by Fourier transform infrared spectroscopy and proton magnetic resonance spectroscopy. Thermally induced polymerization kinetics was investigated using differential scanning calorimetry. Kinetic parameters could be obtained by a dynamic method. The results of these experiments are quite close to first-order reaction for the maleimide double bond polymerization, regardless of the length of the imide end-capped oligomers which can be explained from theory (reaction mechanism) and experiment. Apparent activation energies (E_a) in the range of 101.52–118.09 kJ/mol and pre-exponential factors (K_0) in the range of 1.35×10^9–1.63×10^{11} min^{-1} were obtained.

Keywords: Bismaleimides; End-capped oligomers; Kinetic parameters

1. Introduction

Bismaleimide (BMI) resins are widely applied in multi-layered printed circuit boards and advanced composite materials. However, the major disadvantage of BMI resins is their brittleness. This is because of high cross-link density and the aromatic nature of the BMIs. In order to overcome this problem, thermoplastics are increasingly used in the toughening of BMI resins to improve their brittleness [1–3]. BMIs bearing polysiloxanes were shown to have a very good thermal stability caused by both the imidic structure and ionic nature of Si–O–C bonds [4]. BMIs can be cured by thermal or free radical polymerization to form cross-linked networks [5–7].

Most kinetic investigations were based on the results from C–C bond or short- chain aromatic BMIs with two bismaleimidophenyl groups connected by a central group such as ($-CH_2-$, $-O-$) [8], and $-SO_2-$ [9] etc. In our study, the BMI resin includes a siloxane segment in the main chain. The structural difference between the general BMI and maleimide-terminated poly(dimethylsiloxanes), (MTPDMS), would influence their polymerization behavior. The effects are; the BMIs with a siloxane segment have less chance of molecular collision (2–4 order, owing to long chain), and have a lower activation energy (10%–15%, owing to random-coil nature) than that of the short chain BMIs. Two procedures were used in the measurement of kinetic parameters, i.e. isothermal (time scans) and dynamic (temperature scans) experiments. For thermosetting encapsulants which require a rather high curing temperature, the kinetic parameters can not be obtained accurately from measurements made under isothermal condition (instrumental and experimental factors etc.). The present study is concerned with a rapid (experiment) and accurate (data treatment) estimation procedure for the determination of kinetic parameters by dynamic experiment. In addition, having a series of oligomers with the same chemical structure but different chain lengths between maleimide groups may enable the evaluation of the influence of the chain length on crosslinking reaction.

As a result of the complex nature of thermosetting reactions, Acevedo et al. [6] and Barton et al. [8] derived the kinetics from phenomenological models. In this study, the proposed kinetic mechanism is expected to explain the kinetic models.

2. Experimental

2.1. Materials

Maleic anhydride (Janssen), sodium acetate (Nacalai

* Corresponding author. Tel.: + 886-6-2757575; fax: + 886-6-2344496.

E-mail address: cswang@mail.ncku.edu.tw (W. Chun-Shan)

0032-3861/99/$ - see front matter
PII: S0032-3861(98)00755-1

Table 1
Amino-terminated siloxanes used for these BMI precursors

Diamine code	Molecular weight
ATPDMS1	900
ATPDMS2	1680
ATPDMS3	3000
ATPDMS4	4600

Structural formula:

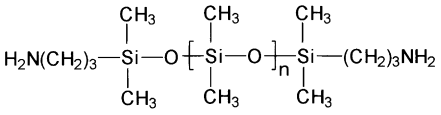

tesque, extra pure reagent), acetic anhydride (Janssen), tetramethylammonium hydroxide (TCI), and the amine-terminated siloxanes were purchased from Shin-Etsu and their structure and molecular weight are shown in Table 1. All other solvents were obtained from various commercial sources and used without further purification.

2.2. Measurements

Differential scanning calorimeter (d.s.c.) (Perkin-Elmer DSC-7) measurements were used in this study. Samples of approximately 6–7 mg in weight were sealed in hermetic aluminum pans and scanned in the calorimeter with a heating rate of 15°C, 20°C, 30°C, and 40°C/min in the range of 40°C–370°C. For dynamic scanning, calibration of the calorimeter was conducted for each heating rate using an indium standard. Fourier transform infrared (F.T.i.r.) spectra were recorded on a Nicolet Magna-520 spectrometer with KBr pellets. Spectra in the optical range of 400–4000 cm^{-1} were obtained by averaging 32 scans at a resolution of 4 cm^{-1}. ^{1}H-NMR spectra were registered using a Bruker Analytik WP-200 spectrometer using DMSO-d_6 as the solvent.

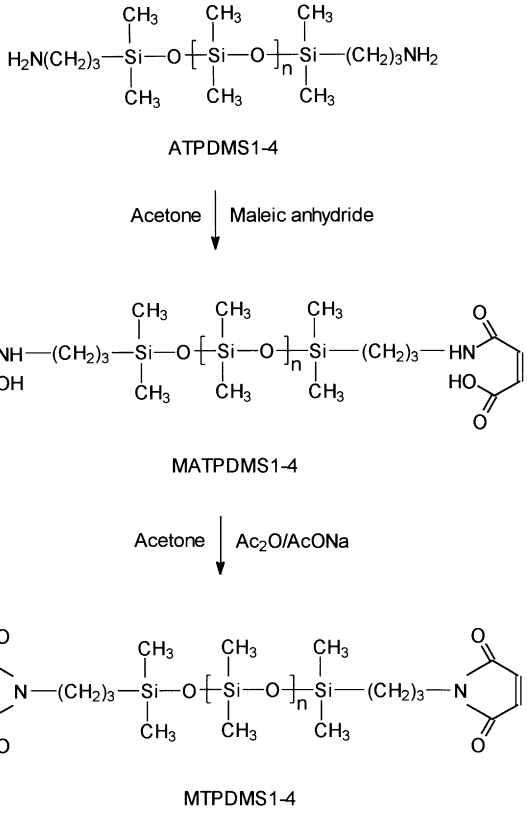

Scheme 1.

2.3. The preparation of maleimide-terminated poly(dimethylsiloxanes)

A three-necked flask equipped with an addition funnel and a nitrogen inlet was charged with a solution of maleic anhydride 3.92 g (0.04 mol) in acetone (12 ml). Under a nitrogen atmosphere, amine-terminated poly(dimethylsiloxane), (ATPDMS1), 16.2 g in acetone (49 ml) was added dropwise to the mixture mentioned earlier. The reaction mixture was stirred at room temperature for 6 h and then at 52°C–54°C for an additional 2 h. Then, the solvent was distilled under reduced pressure to obtain pale-yellow viscous product of maleamic acid-terminated poly(dimethylsiloxane), (MATPDMS).

We added 17.76 g of oligomeric bismaleamic acid (i.e., MATPDMS) and 71 ml of acetone to a 250 ml round-bottomed flask. The solution was heated to 52°C–54°C with stirring. Acetic anhydride 10 ml and 0.9 g of sodium acetate (300 ml and 27 g, respectively per mol of water condensed) [10] were added to the preheated solution. The temperature of the reaction mixture was raised to the reflux temperature and was stirred at that temperature for 10 h. Then the solvent and residual reactants were distilled to give a brown viscous product. The yield of MTPDMS (ca. 92%), IR(KBr) cm^{-1}: 1783, 1718 (imide ring), 703 (maleimide ring), 1390-asym., 1260-sym., 800 (Si–CH_3), 1090 (Si–O–Si); ^{1}H-NMR (200 MHz, DMSO-d_6): δ: 0.45 (m, aliphatic H's ortho to –$Si(CH_3)_2$–), δ: 1.55 (m, aliphatic H's ortho to –CH_2–), δ: 3.15 (m, aliphatic H's ortho to –$N(CO)_2$), δ: 6.38 (m, olefinic H's in imide ring).

3. Results and discussion

3.1. Synthesis of oligomers and analysis

Scheme 1 shows the synthetic routes to MTPDMSs. MTPDMSs were prepared from the corresponding maleamic acid using acetic anhydride in the presence of a catalytic amount of sodium acetate at specific temperature [11]. Four MTPDMSs were obtained from ATPDMS1-4 (i.e. Mw: 900–4600). The BMI showed a strong absorption at 1718 cm^{-1} and a weak absorption at 1783 cm^{-1}, assigned to asymmetric and symmetric C=O stretching vibration of

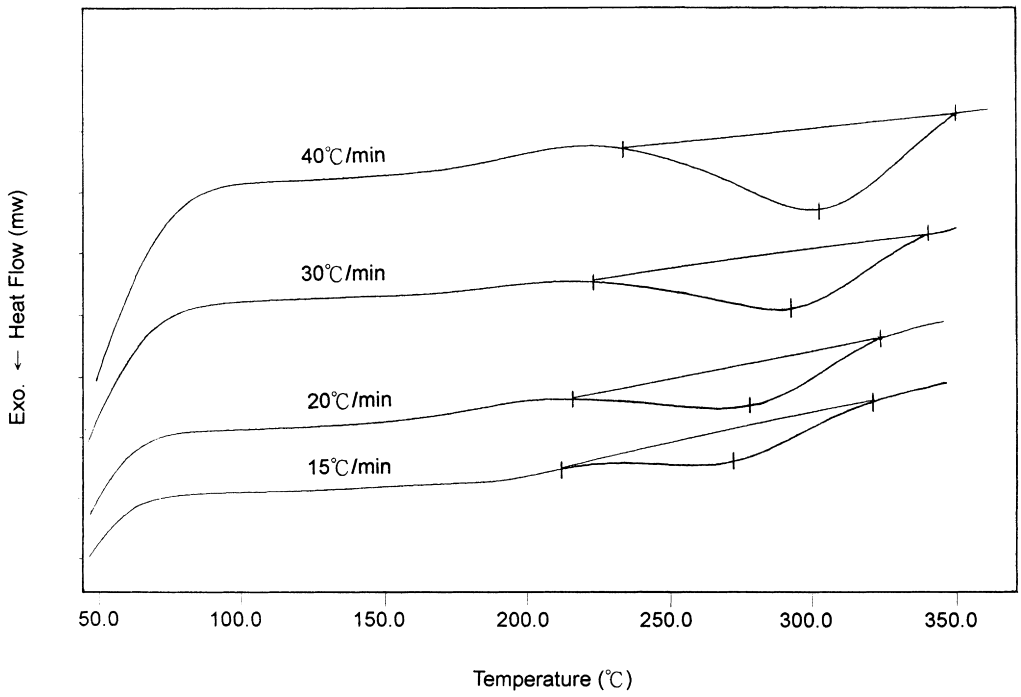

Fig. 1. D.s.c. curves of MTPDMS1 at various heating rates, the baseline was determined from the horizontal straight method.

imide ring respectively, it also lacked the absorption at 3200–3400 cm^{-1} associated with the carboxylic OH stretching vibration and 1540 cm^{-1} for the NH stretching of the amide group. Consequently, imidization could be monitored by means of this absorption. The number-average molecular weights of the maleimide-terminated oligomers (i.e., MTPDMSs) were estimated by two methods: First by the ratio of $-Si(CH_3)_2-$ protons (δ:0.15) to $-(CH_2)_3$ protons (δ: 0.45) in ^{1}H-NMR [12–13]. Secondly, by the acid–base potentiometric titration of the corresponding bismaleamic acid. A solution of tetramethylammonium hydroxide dissolved in absolute methanol was used as titrant. The samples were dissolved in methanol, and the end points were detected by the first derivative of the potential vs. volume of titrant. The number-average molecular

Table 2
Peak temperature (T_p) and peak conversion (X_p) at different heating rates (Φ) of MTPDMSs (1–4)

Sample code	Φ (°C/min)	T_p[a] (°C)	X_p[b] (%)	ΔH_p[c] (kJ/mol)	E_a[d] (kJ/mol)
MTPDMS1	15	268.63	55.7	35.73	117.53
	20	272.48	55.8		
	30	281.41	52.1		
	40	289.35	52.4		
MTPDMS2	15	294.19	54.5	27.16	114.69
	20	301.95	55.8		
	30	304.87	54.5		
	40	317.32	55.5		
MTPDMS3	15	295.32	51.3	24.40	108.56
	20	302.68	50.1		
	30	311.80	54.2		
	40	318.23	52.0		
MTPDMS4	15	296.47	54.5	30.13	100.16
	20	303.70	54.8		
	30	316.97	52.1		
	40	321.18	51.9		

[a] Temperature at maximum rate of reaction.
[b] The corresponding conversion at peak temperature.
[c] Heat of polymerization (average values).
[d] Apparent activation energy (from Prime's equation).

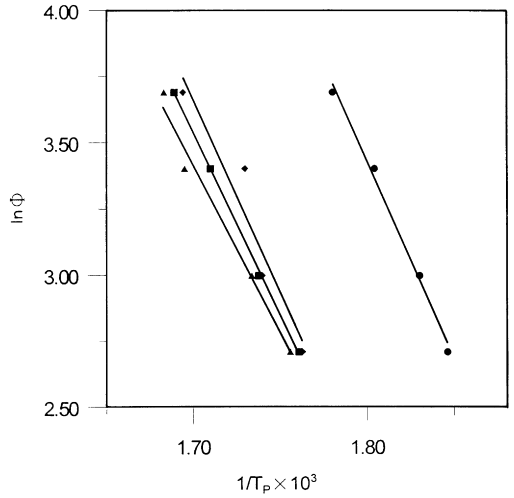

Fig. 2. Plots of lnΦ vs. $1/T_p$ for (●: MTPDMS1, ◆: MTPDMS2, ■: MTPDMS3, ▲: MTPDMS4).

weights of oligomers were almost identical for both determinations.

3.2. Thermal behaviors

The thermal behaviors of all four samples were investigated by d.s.c., the representative dynamic d.s.c. traces of MTPDMS1 at various heating rates are shown in Fig. 1. No peak in front of a polymerization exotherm was observed in the d.s.c. scans, this may be attributed to the amorphous molecular structure, and the polymerization exotherms were broad. In addition, curing reactions for all samples can be safely completed below 380°C without decomposition during curing. The subsequent heating after quenching these samples from 400°C showed no traces of an exotherm, indicating that curing reaction was completed during the dynamic d.s.c. scan.

3.3. Cure kinetics

The general mathematical model to describe the kinetics of a system undergoing chemical change is

$$\frac{dx}{dt} = k(T)\, f(x), \tag{1}$$

where x is the degree of cure, dx/dt the rate of reaction. From Eq. (1), it can be seen that the rate is both a function of temperature, given by $k(T)$ and a function of the degree of conversion, given by $f(x)$. The rate of reaction corresponds to the height (with respect to the base line) of the d.s.c. curve at a given temperature, $k(T) = k_0 \exp(-E_a/RT)$ is the apparent rate constant, k_0 the pre-exponential factor, and E_a the apparent activation energy. The reaction rate curves at the peak maximum (T_p) is defined by [14].

$$\left[\frac{d(dx/dt)}{dT}\right]_{T_p} = 0. \tag{2}$$

From Eq. (2), it was observed that the extent of reaction at the peak temperature (T_p) is a constant (i.e. maximum value) and independent of the heating rate for many thermosetting systems [15]. Integration of $1/f(x)$ from $x = 0$ to x_p (peak conversion; the corresponding conversion at peak temperature) should yield a constant value and the following relationship was reduced by Prime [16],

$$E_a = -0.951R\frac{d\ln \Phi}{d(1/T_p)}. \tag{3}$$

If the resulting extent of reaction at the peak temperature would change with the heating rate, it would be improper to use Eq. (3). In addition, the data adapted from the dynamic d.s.c. runs of all samples are summarized in Table 2. The specific heat of the cure reaction (ΔH_p, kJ/mol) and apparent activation energy (E_a, kJ/mol) were clearly decreased with increasing molecular weight, owing to the reduced concentration of maleimido groups. The high E_a for low molecular weight was resulting from its short-chain character which limits the segmental motions of the curing material; also, Flory [17] had suggested persuasively that the random coil model promoted the rotation of polymer chains, and the distribution of end-to-end distances can be treated by Gaussian distribution functions. The relatively constant peak conversion (x_p) irrespective of the heating rate (Φ) ensures that Eq. (3) can be used to evaluate the apparent activation energy. Plots of lnΦ vs. $1/T_p$ for all samples are given in Fig. 2. Like in most kinetic studies, the Arrhenius equation is used for expressing the temperature dependence of $k(T)$, Eq. (1) now becomes

$$\frac{dx}{dt} = k_0\, f(x)\cdot\exp(-E_a/RT), \tag{4}$$

where $f(x)$ is an empirical function representing the conversion-dependent part of the rate expression. An approach to survey E_a throughout the entire conversion range can be obtained by using Friedman's method [18]. When E_a is taken as a constant, Eq. (4) can be rewritten as

$$\ln\frac{dx}{dt} = \ln[k_0\, f(x)] - E_a/RT. \tag{5}$$

According to Eq. (5), for the conversion from $x = 0.1$ to 0.9, the plot of $\ln(dx/dt)$ against reciprocal of absolute temperature at a selected conversion should yield a straight line with its slope (E_a) and intercept [$k_0 f(x)$]. The E_a values

Table 3
Crosslinking kinetic parameters of MTPDMSs obtained from the non-isothermal runs

Sample code	E_a[a] (kJ/mol)	K_0[b] (min^{-1})
MTPDMS1	118.09	1.63×10^{11}
MTPDMS2	116.61	4.10×10^{10}
MTPDMS3	110.31	9.05×10^{9}
MTPDMS4	101.52	1.35×10^{9}

[a] Average apparent activation energy.
[b] Average pre-exponential factor (from Friedman's method).

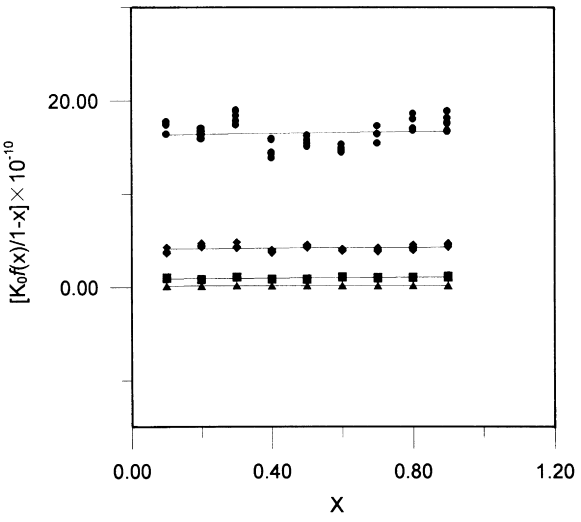

Fig. 3. Plots of $k_0 f(x)1 - x$ vs. x for (●: MTPDMS1, ◆: MTPDMS2, ■: MTPDMS3, ▲: MTPDMS4).

for the present system were observed to fluctuate with conversion, and the complex nature of the cure system is revealed by the scattered E_a values (e.g. diffusion, mobility, etc.). The value of $[k_0 f(x)]$ in Eq. (5) can be calculated from the experimentally determined dx/dt and E_a. For a multiple bond polymerization, nth-order kinetics has always been reported. Hence, the simple nth order model is

$$\frac{dx}{dt} = k(1-x)^n, \tag{6}$$

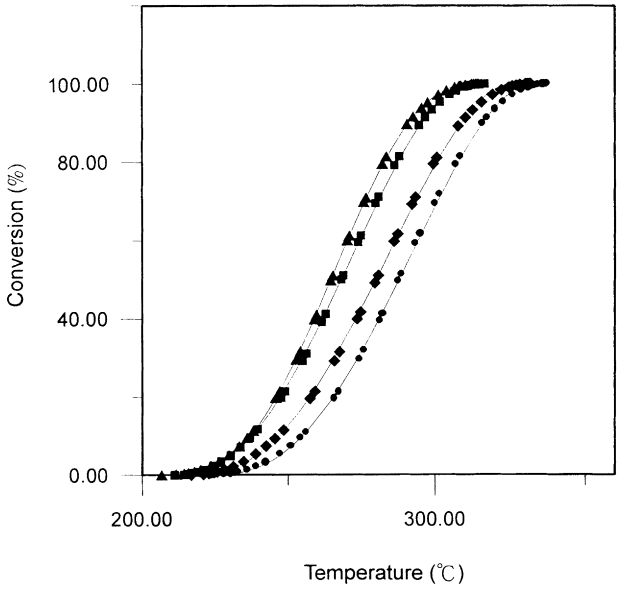

Fig. 4. Comparison between experimentally determined conversion (symbols) and the curves (solid lines) evaluated from the empirical rate expressions (i.e. Eq. 13 combining with Eq. 17). The corresponding heating rates are from left to right (15, 20, 30 and 40°C min^{-1}).

where k is the rate constant, and taking its logarithmic form

$$\ln\frac{dx}{dt} = \ln k_0 - E_a/RT + n\ln(1-x). \tag{7}$$

Combining Eqs. (5) and (7), we obtain

$$\ln[k_0 f(x)] = \ln k_0 + n\ln(1-x). \tag{8}$$

The plot of $\ln[k_0 f(x)]$ vs. $\ln(1-x)$ for over the range of conversion, gives better agreement for the first-order model. Moreover, the E_a and k_0 values obtained in this case (using Friedman's method) are summarized in Table 3. The resulting apparent activation energies using the two methods (i.e. Prime and Friedman) were quite close. The results indicated that the curing temperature increases with the size of bridging group between two maleimido end caps (mathematically, a higher temperature, and therefore a higher $\exp(-E_a/RT)$ term, would be required to compensate for its lower pre-exponential factor, k_0). It resulted in lower pre-exponential factor for MTPDMS4 as compared with other samples (MTPDMS1-3).

Fitting the resulting $k_0 f(x)$ value with x resulted in the possible kinetics form. As shown in Fig. 3, the plot of $[k_0 f(x)/1\text{-}x]$ vs. x resulted in a straight line, indicating a plausible autocatalytic first-order kinetics for curing of four samples. The resulting rate expressions can be formulated as follows;

$$k_0 f(x) = 1.63\times10^{11}(1 + 0.0245x)(1-x) \tag{9}$$

(for MTPDMS1),

$$k_0 f(x) = 4.10\times10^{10}(1 + 0.0561x)(1-x) \tag{10}$$

(for MTPDMS2),

$$k_0 f(x) = 9.05\times10^{9}(1 + 0.2111x)(1-x) \tag{11}$$

(for MTPDMS3),

$$k_0 f(x) = 1.35\times10^{9}(1 + 0.2815x)(1-x) \tag{12}$$

(for MTPDMS4).

The equations aforementioned can be written in a conversion-dependent term as $f(x) = (1 + k_a x)(1-x)$, where k_a is an empirical constant, as $k_a x \ll 1$. Thus, Eqs. (9)–(12) can be reduced to

$$k_0 f(x) = 1.63\times10^{11}(1-x), \tag{13}$$

$$k_0 f(x) = 4.10\times10^{10}(1-x), \tag{14}$$

$$k_0 f(x) = 9.05\times10^{9}(1-x), \tag{15}$$

$$k_0 f(x) = 1.35\times10^{9}(1-x). \tag{16}$$

Temperature integration can be achieved by using the derivative (dT/dt = Φ) in Eq. (4), and can be written in

a. Chain reaction

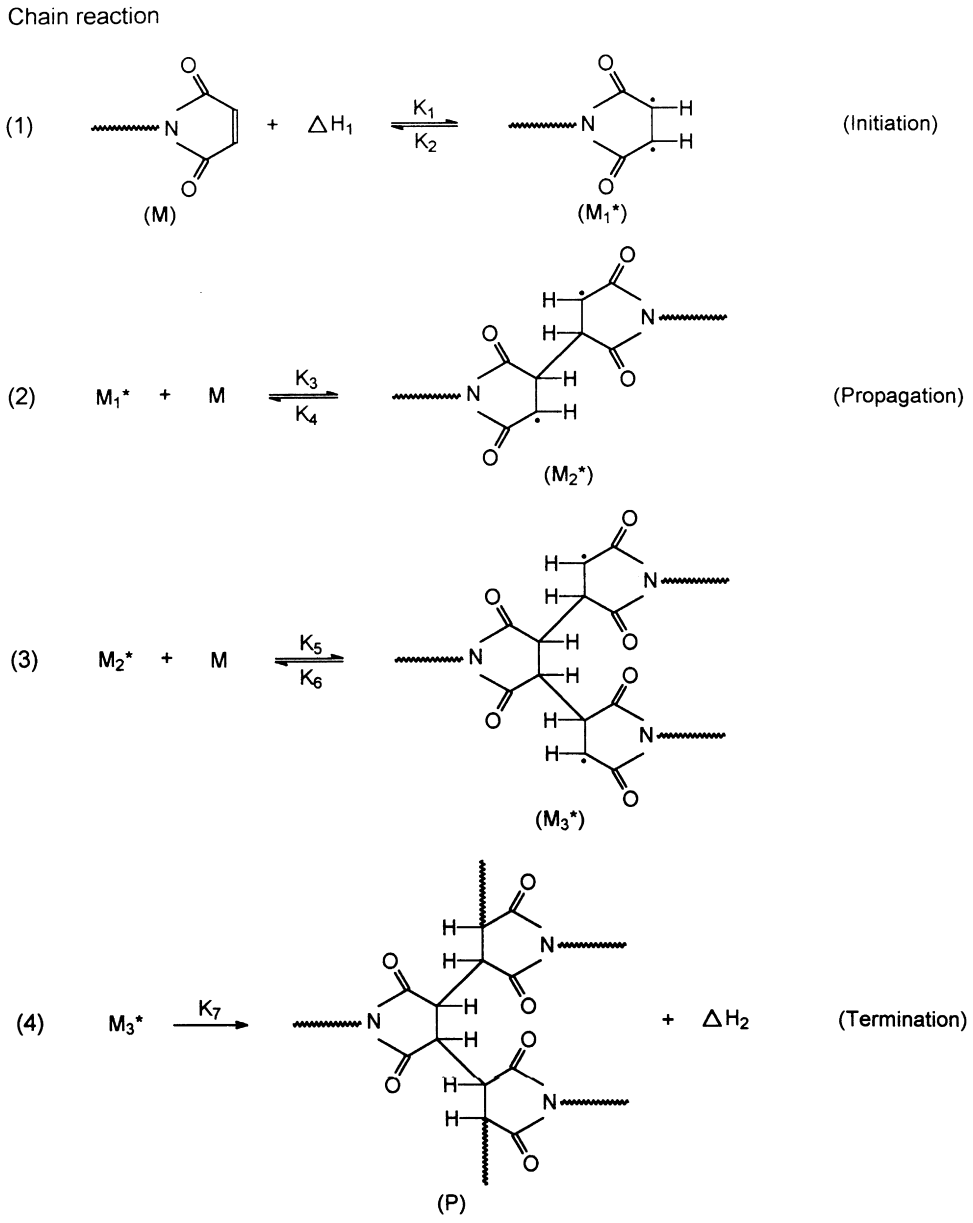

b. Nonchain reaction

(5) $M + \Delta H_1 \underset{K_2}{\overset{K_1}{\rightleftharpoons}} M^*$

(6) $M^* + M \xrightarrow{K_3} P + \Delta H_2$

Scheme 2.

the following integrated form

$$\int_0^x \frac{dx}{k_0 f(x)} = \frac{1}{\Phi} \int_{T_0}^{T} \exp(-E_a/RT)\, dT. \quad (17)$$

Then, simulation of the theoretical curves vs. T, using the evaluated E_a and $k_0 f(x)$ (from known conversion function of Eqs. (13)–(16)) values, by numerical integration of Eq. (17) [6,19,20] yields a conversion–temperature curve. The calculated curves correlate well with the experimental results, as shown in Fig. 4 for MTPDMS1. A similar situation holds for other samples also.

3.4. Kinetic mechanism and rate equation

The first-order kinetics for homopolymerization can be

a. Chain reaction:

$$R_{M_1^*} = 0 = K_1[M] - K_2[M_1^*] - K_3[M][M_1^*] + K_4[M_2^*]$$

$$[M_1^*] = \frac{K_1[M] + K_4[M_2^*]}{K_2 + K_3[M]}$$

$$R_{M_2^*} = 0 = K_3[M][M_1^*] - K_4[M_2^*] - K_5[M][M_2^*] + K_6[M_3^*]$$

$$[M_2^*] = \frac{K_3[M][M_1^*] + K_6[M_3^*]}{K_4 + K_5[M]} \quad (18)$$

$$R_{M_3^*} = 0 = K_5[M][M_2^*] - K_6[M_3^*] - K_7[M_3^*]$$

$$[M_3^*] = \frac{K_5[M][M_2^*]}{K_6 + K_7}$$

From (18)

$$[M_2^*] = \frac{K_1K_3[M]^2}{K_5K_7[M](K_2 + K_3[M])} \quad (K_4 \text{ and } K_6 \text{ are very small})$$

$$R_P = K_7[M_3^*] = \frac{K_1K_3[M]^2}{K_2 + K_3[M]}$$

b. Nonchain reaction

$$R_{M^*} = 0 = K_1[M] - K_2[M^*] - K_2[M][M^*]$$

$$[M^*] = \frac{K_1[M]}{K_2 + K_3[M]}$$

$$R_P = K_3[M][M^*] = \frac{K_1K_3[M]^2}{K_2 + K_3[M]}$$

Scheme 3.

understood by the mechanistic steps illustrated in Scheme 2. To explain the kinetics of non-elementary reactions we assume that a sequence of elementary reactions is actually occurring but that we cannot measure or observe the intermediates formed, thus we observe only the initial reactants and final products (e.g. non-chain reaction). From the reaction mechanisms shown in Scheme 3 (ΔH_1: endothermic enthalpy, δ-bond cracked in imide ring and ΔH_2: exothermic enthalpy, π-bond arranged on imide ring; $\Delta H = \Delta H_1 + \Delta H_2 < 0$, because the 2nd law of thermodynamics must be obeyed), both chain and non-chain reactions resulted in the same rate equation expression:

$$R_p = \frac{k_1k_3[M]^2}{k_2 + k_3[M]}. \quad (19)$$

The resulting mechanisms derived to an identical equation for chain and non-chain reaction, where K_1, K_2 and K_3 are rate constants, [M] represents the concentration of the oligomer (i.e. MTPDMS). Thus, if K_2 is very small, this expression reduces to

$$R_p = k_1[M]. \quad (20)$$

We were fortunate in this case to have represented our data in an equation which happened to match exactly with what was obtained from the theoretical mechanism.

4. Conclusion

The isothermal technique typically covers a limited temperature and is dependent of the activation energy of reaction and instrumental factors (i.e. sensitivity and stability). Conversely, a temperature scan covers a much wider temperature range in excess of 90°C, the system undergoes large viscosity increase and changes in state from viscous liquid through gel to glass. Despite the molecular weight difference, a first-order kinetics expressed by $dx/dt = k_0(1-x)\exp(-E_a/RT)$ can be used to describe the curing reaction of the four MTPDMSs prepared in this study. The pre-exponential factor (k_0) and apparent activation energies (E_a) tend to be lower with increasing molecular weight. BMIs bearing polysiloxanes have the flexible segments (Si–O) and long-chain character in the backbone. As a result of their structure characteristics (possessing ionic nature and high intramolecular force), their curing kinetics, i.e. polymerization behavior is quite different from the general BMI resin. The study of the crosslinking reaction reveals that the proposed kinetic mechanism is in good agreement with the kinetic models.

References

[1] Lyle GD, Senger JS, Chen DH, Kilic S, Wu SD, Mohanty DK, McGrath JE. Polymer 1989;30:978.
[2] Taleda S, et al. J Appl Polym Sci 1988;35:1341.
[3] Acevedo M, et al. J Appl Polym Sci 1989;38:1745.
[4] Laurienzo P, Malinconico M, Perenze N, Segne AL. Macromol Chem Phys 1994;195(5):3057.
[5] Brown IM, Sandreczki TC. Macromolecules 1990;23:100.
[6] Acevedo M, Abajo J, de la Campa JG. Polymer 1990;31:1955.
[7] Pan JP, Shian GY, Lin SS, Chen KM. J Appl Polym Sci 1992;45:103.
[8] Barton JM, Hamerton I, Rose JB, Warner D. Polymer 1992;33(17):3664.
[9] Varma IK, Sharma S. Polymer 1985;26:1561.
[10] Wang CS, Hwang HJ. Polymer 1996;37:499.
[11] Stenzenberger HD. In: Wilson D et al., editors. Polyimides. Glasgow/London: Blackie, 1990:79.
[12] Racles C, Gaina V, Marcu M, Cazacu M, Simionescu M. JMS Pure Appl Chem 1997;A34(9):1605.
[13] Chang JY, Hong JL. Macromol Chem Phys 1995;196:3753.
[14] Ryan ME, Dutta A. Polymer 1979;20:203.
[15] Hsieh TH, Su AC. J Appl Polym Sci 1990;41:1271.
[16] Prime RB. Polym Eng Sci 1973;13:365.
[17] Flory PJ. Principles of polymer chemistry. Ithaca, NY: Cornell University Press, 1953.
[18] Friedman HL. J Polym Sci Part C 1965;6:183.
[19] Gebben B, Mulder MH, Smolders CA. J Polym Sci Chem Edn 1988;26:1743.
[20] Riccardi CC, Adabbo HE, Williams RJ. J Appl Polym Sci 1984;29:2481.